Analysis and modelling of the magnetic and plasma profiles during PPCD experiments in RFX

To cite this article: M.E. Puiatti *et al* 2003 *Nucl. Fusion* **43** 1057

INSTITUTE OF PHYSICS PUBLISHING and INTERNATIONAL ATOMIC ENERGY AGENCY NUCLEAR FUSION

Nucl. Fusion **43** (2003) 1057–1065 PII: S0029-5515(03)67567-8

Analysis and modelling of the magnetic and plasma profiles during PPCD experiments in RFX

M.E. Puiatti, S. Cappello, R. Lorenzini, S. Martini, S. Ortolani, R. Paccagnella, F. Sattin, D. Terranova[1], T. Bolzonella, A. Buffa[1], A. Canton[1], L. Carraro, D.F. Escande, L. Garzotti, P. Innocente, L. Marrelli, E. Martines, P. Scarin, G. Spizzo[1], M. Valisa, P. Zanca, V. Antoni[1], L. Apolloni, M. Bagatin[1], W. Baker, O. Barana, D. Bettella, P. Bettini, R. Cavazzana, M. Cavinato, G. Chitarin, A. Cravotta, F. D'Angelo, S. Dal Bello, A. De Lorenzi, D. Desideri[1], P. Fiorentin, P. Franz, L. Frassinetti[1], E. Gaio, L. Giudicotti[1], F. Gnesotto, L. Grando, S.C. Guo, A. Luchetta, G. Malesani, G. Manduchi, G. Marchiori, D. Marcuzzi, P. Martin[1], A. Masiello, F. Milani, M. Moresco[1], A. Murari[1], P. Nielsen, R. Pasqualotto[1], B. Pégourie[2], S. Peruzzo, R. Piovan, P. Piovesan[1], N. Pomaro, G. Preti, G. Regnoli, G. Rostagni, G. Serianni, P. Sonato, E. Spada, M. Spolaore, C. Taliercio, G. Telesca[3], V. Toigo, N. Vianello, P. Zaccaria, B. Zaniol[1], L. Zanotto, E. Zilli[1], G. Zollino and M. Zuin[1]

Consorzio RFX, Associazione EURATOM-ENEA sulla Fusione, Padova, Italy
[1] INFM Istituto Nazionale Fisica della Materia, Unità di Padova, Italy
[2] Association EURATOM-CEA sur la Fusion Controlée, CEA-Cadarache, France
[3] LPP-ERM/KMS Euratom—Belgium State Association, Brussells, Belgium

E-mail: puiatti@igi.pd.cnr.it

Received 14 November 2002, accepted for publication 11 August 2003
Published 4 September 2003
Online at stacks.iop.org/NF/43/1057

Abstract
In this paper, we analyse the main features of the pulsed poloidal current drive (PPCD) technique, used in the reversed field pinch configuration to achieve improved confinement conditions. In the RFX experiment, PPCD corresponds to a decrease of the magnetic fluctuations, to a peaking of the temperature profile, and to a reduced transport and plasma–wall interaction. A three-dimensional MHD nonlinear code and one-dimensional time-dependent transport models have been applied to study the effect of PPCD on the magnetic and plasma profiles. The three-dimensional MHD simulations show that the external inductive drive pinches and peaks the current profile driving the configuration through a transient phase, where the spontaneous turbulent dynamo action is quenched. The one-dimensional transport codes indicate that the experimental profile modifications associated with PPCD are consistent with a reduction of the stochastic transport.

PACS numbers: 52.55.Hc, 52.25.Fi, 52.30.Cv, 52.35.Mw

1. Introduction

The reversed field pinch (RFP) is a magnetic configuration whose symmetry is broken by unstable $m = 1$ resistive MHD modes. These modes generate electric fields producing a drift velocity field and consequently a $[\boldsymbol{v} \times \boldsymbol{B}]$ dynamo field that can maintain the profiles in steady state against resistive diffusion. In standard discharges in the RFX experiment these dynamo modes have a strong influence on the transport mechanism governing both the centre and the edge of the plasma [1]. In the core, roughly corresponding to the region inside the magnetic toroidal field reversal surface (where $q = 0$, at $r/a \sim 0.9$), transport is driven by parallel transport in a stochastic magnetic field [2]. The magnetic turbulence causing the magnetic field stochastization is due to the wide spectrum of $m = 1, n = 7$–15 modes resonating inside the $q = 0$ surface (a regime dubbed multiple helicity or MH). In some cases, a spontaneous transition to an MHD spectrum dominated by a single, low n, $m = 1$ mode has been observed (a regime dubbed QSH for quasi-single helicity [3]). At the edge, electrostatic fluctuations are an important loss channel [4], but more than 50% of the power losses have been associated with localized plasma–wall interaction due to the non-axisymmetric magnetic perturbations caused by locked dynamo modes [5, 6].

Techniques to improve confinement have been developed. In particular a better quality of the magnetic configuration can be achieved by transiently applying a pulsed current in the toroidal field coils.

The rationale of the pulsed poloidal current drive (PPCD) that emerges from the analysis presented here is that when poloidal currents are inductively driven at the plasma edge and the system is in a non-stationary state, the need for the dynamo is quenched and the adverse effect of the dynamo modes on magnetic stochasticity is reduced.

PPCD experiments have been performed in various RFP devices [1, 7–9], resulting in an increase of the core electron temperature and a reduction of transport through the reduction of the magnetic fluctuations. PPCD has beneficial effects also on the edge properties, since reduction of the dynamo modes entails a smaller localized perturbation of the magnetic surfaces, resulting in a more uniform plasma–wall interaction and in a reduction of direct parallel losses along field lines intercepting the vessel.

The aim of this paper is to study the effect of PPCD on the magnetic and plasma profiles in RFX and the related decrease of the transport. In section 2, an overview of the main experimental observations during PPCD is given; in section 3, a three-dimensional MHD simulation of the PPCD provides a confirmation of the direct link between the technique and the observed reduction of the magnetic fluctuations and highlights some new features of the mechanism. One-dimensional transport simulations show the achievement of an enhanced confinement regime associated with suppression of the spontaneous dynamo action when PPCD is applied (section 4). In section 5, some perturbative transport studies with pellet injection confirm the robustness of the technique and the possibility of improving its effectiveness in terms of confinement enhancement by means of active density control. The summary and conclusions are given in section 6.

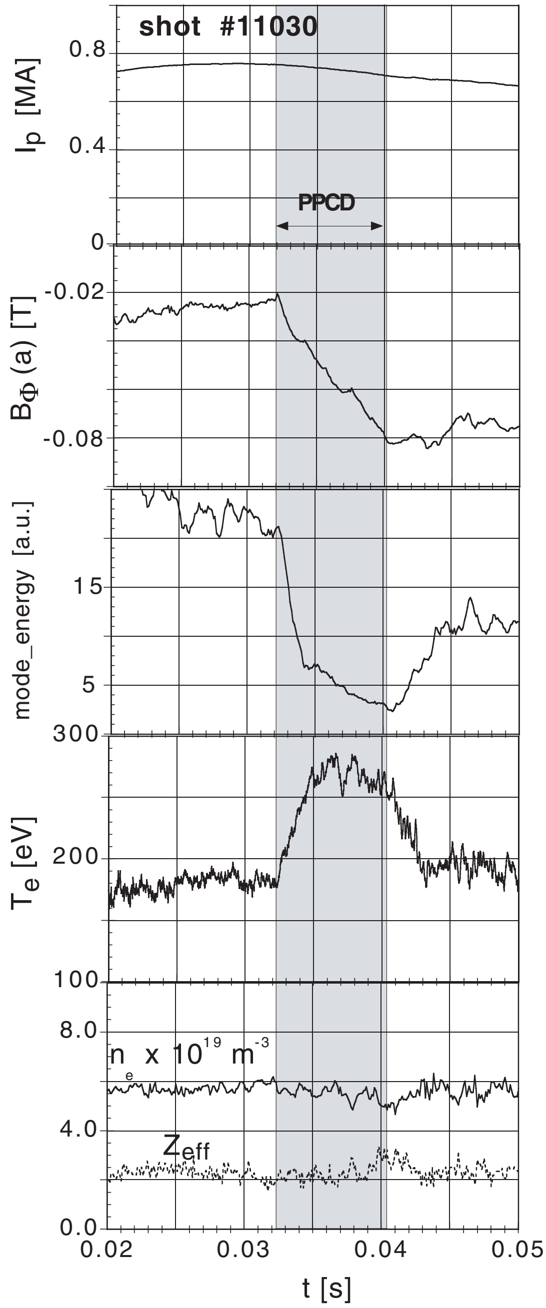

Figure 1. Main plasma parameters during PPCD (shadowed region) from top to bottom: plasma current, toroidal field at the wall, normalized total mode energy, electron temperature, electron density, and effective charge.

2. Summary of experimental observations

To recall the main features of a PPCD experiment in RFX, the time evolution of typical plasma parameters is shown in figure 1. It clearly evidences the reduction of the total mode energy and the increase of the on-axis electron temperature in the initial phase of PPCD, when the edge toroidal magnetic field is driven more negative. It has to be mentioned that the behaviour of the electron temperature and of the mode energy are not fully reproducible. For example, regarding the mode energy, there are two main sets of situations in which it either decreases or even increases, when a QSH occurs. A more exhaustive discussion about this point can be found in [10]. In this paper, the experiments featuring both a significant increase of the temperature and a decrease of the turbulent dynamo activity will be discussed.

According to a standard axisymmetric equilibrium reconstruction, the deepening of the edge toroidal field produced by PPCD results in an inward displacement of the reversal surface and a peaking of the current profile in the central region.

The edge behaviour is also influenced by PPCD. Measurements performed at a low plasma current, ~300 kA, show a reduction of the particle and thermal fluxes driven by electrostatic fluctuations at the edge [11]. It has been observed that the cause of this decrease of electrostatic transport is not related to an increase of the shear of the edge radial electric field, E_r, which is actually reduced. A decrease of E_r at the edge has been observed also at higher current, ~800 kA, through measurement of the plasma rotation velocity from the Doppler shift of C III spectral lines (C III is localized in the last 3–5 cm of the plasma radius). Indeed, the rotation velocity, proportional to E_r if the edge density and temperature do not change, decreases when PPCD is applied. Different mechanisms, such as a shrinking of the plasma column, have been suggested in [11] to explain the reduction of fluxes at the edge.

A picture of reduced edge transport is consistent with the simulation of the impurity behaviour during PPCD by a one-dimensional impurity diffusion model. To reconstruct the radiation experimental scenario, the edge region of low diffusion found in stationary conditions has to be broadened, as shown in figure 2 and discussed in [12].

One of the beneficial effects of PPCD is the mitigation of non-axisymmetric magnetic perturbation due to the locked dynamo modes. Indeed, the reconstruction of the last closed magnetic surface shows that PPCD reduces its maximum localized radial displacement from ~2–4 to ~1 cm (figure 3). As a result of this less severe plasma–wall interaction, both hydrogen and impurity influxes decrease drastically at the locking position. Figure 4 shows the time evolution of the H_α line at the position where modes are locked during a PPCD experiment. Since this local contribution to the total influx has been evaluated to be about 50% (both for hydrogen and impurities) [5], a strong reduction in the locking region leads to a decrease of the total H and impurity source by up to a factor of 2.

As previously reported [13, 14], in RFX a strong decrease of the magnetic fluctuations is observed during PPCD. Moreover, the timescale of the magnetic mode amplitude reduction is of the order of 1 ms and from recent analysis it has been observed that the most internal $m = 1$ modes ($n = 7$–8) decrease simultaneously or just before the more external ones (figure 5). Such a behaviour cannot be simply explained in terms of resistive diffusion since in that case a longer delay would be expected before the core resonant $m = 1$ modes could be affected.

When the temperature increase during PPCD is above 40%, in most cases a helical thermal structure is observed by soft x-ray (SXR) tomography and by Thomson scattering (TS) [10, 15]. By simultaneous analysis of TS profiles and data from a double filter SXR system, it is possible to discriminate the temperature inside and outside the localized structure, concluding that in any case the temperature on axis increases (figure 1) and the profile peaks during the transient phase of PPCD. To summarize the temperature behaviour, a comparison of the profiles obtained by TS in discharges with and without

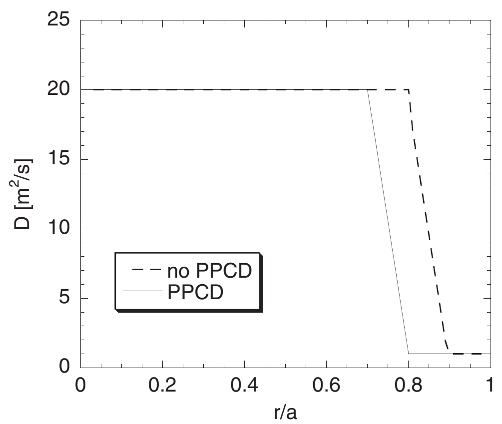

Figure 2. Variation of the impurity diffusion coefficient associated with PPCD.

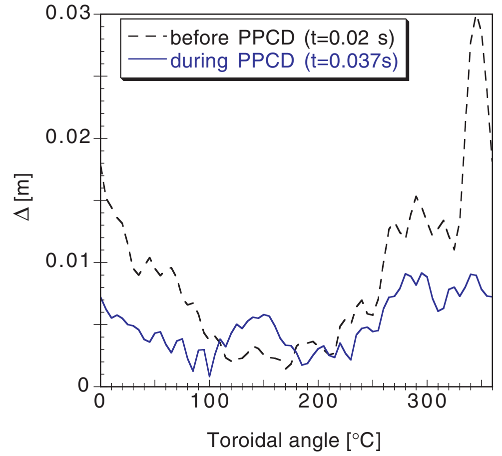

Figure 3. Localized radial displacement before and during PPCD as a function of the toroidal angle.

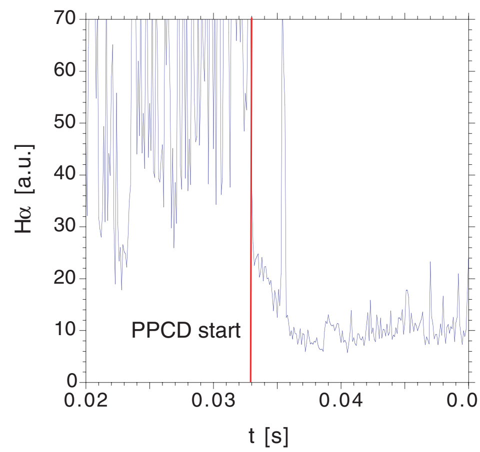

Figure 4. Time evolution of the H_α brightness (representative of the hydrogen influx) during PPCD at the toroidal position where $m = 1$ modes are locked.

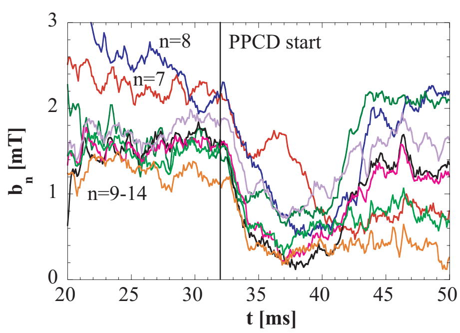

Figure 5. Time evolution of the $m = 1$, $n = 7$–14 magnetic modes during PPCD.

PPCD is shown in figure 6, where the data are ensembles of many reproducible shots.

The behaviour of the electron density is quite different. In RFX the time evolution of the profiles is measured by a 13 chord MIR interferometer [16]: the central chord value decreases during PPCD, while the profile is usually hollow before the start of PPCD experiments and does not change significantly. An example is shown in figure 7, where the experimental line-integrated data and the corresponding inverted profiles before and during PPCD are reported.

Despite the reduction of the influxes, the plasma effective charge, Z_{eff}, from the continuum bremsstrahlung emission remains about constant or in some cases increases slightly during PPCD (figure 1), mainly because of the decrease of the electron density and a higher ionization degree, associated with the higher temperature.

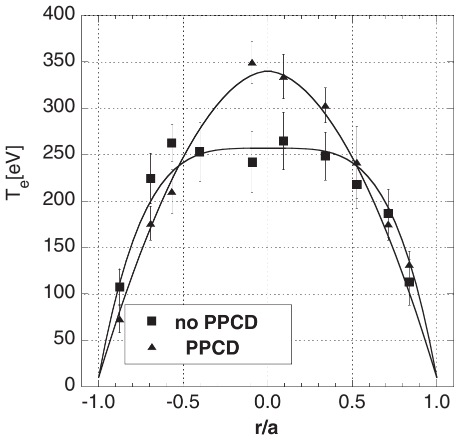

Figure 6. Comparison of the electron temperature profiles as obtained in discharges without PPCD and during PPCD. Data are ensembles of many reproducible shots.

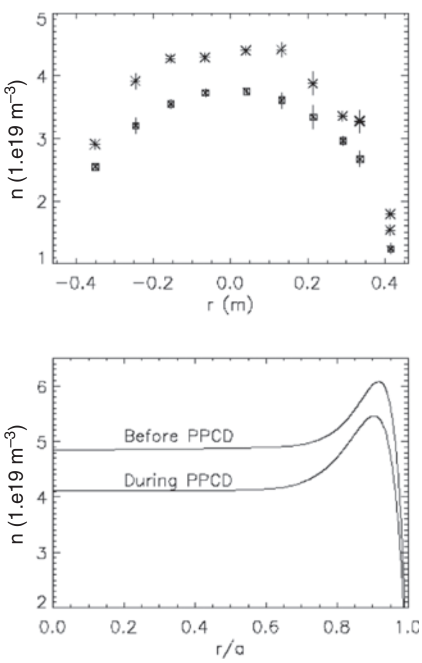

Figure 7. Experimental density profiles before and during PPCD: top frame shows line average electron densities measured along 13 chords (some chords have the same impact parameter); bottom frame show the profiles computed by the inversion code.

3. Three-dimensional MHD simulations

A PPCD experiment has been simulated by means of a three-dimensional MHD non linear code (SpeCyl). The PPCD external drive is applied as a boundary condition with a prescribed decrease in time of toroidal magnetic field at $r = a$, instead of the standard condition of constant toroidal magnetic flux [17]. Constant poloidal magnetic field and initial conditions of MH at $\Theta = 1.6$ have been used. The Lundquist number is $S = 3 \times 10^4$ ($\sim 10^6$ in the experiment). As in the experiment, the typical evolution of PPCD corresponds to characteristic times of the external action several orders of magnitude larger than the Alfven timescale ($\tau_{\mathrm{PPCD}} \sim 10^3 \tau_{\mathrm{A}}$ in RFX, $\sim 10^2 \tau_{\mathrm{A}}$ in simulation) and much lower than the resistive time ($10^{-3} \tau_{\mathrm{R}}$ both in experiment and simulations). Two values for the Prandtl number (ratio between the viscous and resistive timescales) have been considered ($P = 1, 20$). Figures 8–11 show the behaviour of some relevant quantities for one representative simulation case in standard adimensional units [17]. In general, as with the experiments, this set of cases shows a significant reduction of magnetic perturbation energy (both as volume content and edge values), which is accompanied by a concentration and shrinking of the magnetic profiles. Figure 8 shows the temporal behaviour of the reversal parameter and of the magnetic perturbation energy for a standard sustainment and an example of PPCD simulation. In the simulation a sort of saturation in the decrease of the perturbation energy, δE^{M}, is found, despite the persistence of the external action. In figure 9 the profiles of toroidal current density $J_z(r)$, $\mu(r) = J \cdot B / B^2$, and radial pinch velocity $v_r(r)$, before (dotted curves) and at the end (plain line) of the PPCD action are compared, showing during PPCD a profile concentration in all the magnetic quantities, with an increase of the pinch velocity, v_r.

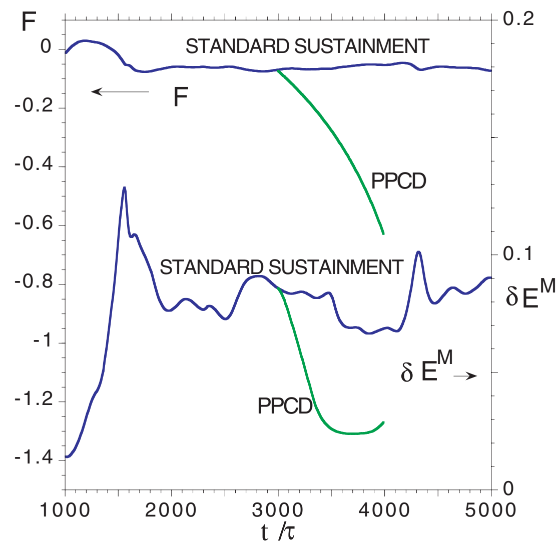

Figure 8. Reversal parameter $F = B_\Phi(a)/\langle B_\Phi \rangle$ and magnetic perturbation energy as obtained from the three-dimensional MHD code. The simulation of a standard sustainment is shown for comparison (time is normalized to the Alfven time).

A simulation has also been done prescribing a temporal variation of resistivity resembling typical experimental behaviour in RFX. The resulting magnetic profiles are negligibly affected, although in this case v_r displays a milder variation.

Regarding the evolution of the dynamo terms, figures 10(*a*) and (*b*) show at the beginning and at the end of PPCD the components of the poloidal electric field along the radius. This quantity accounts for the toroidal flux variation inside a surface of radius r:

$$E_\Theta(r) = [\eta J_\Theta + v_r B_z - \langle \delta v \times \delta B \rangle_\Theta] = -\frac{1}{2}\pi r \left(\frac{\mathrm{d}\phi(r)}{\mathrm{d}t} \right).$$

In particular we display the total $E_\Theta(r)$ and its three terms related, respectively, to the diffusion, pinch velocity (laminar dynamo), and fluctuating fields (turbulent dynamo). At the beginning of PPCD the plasma is almost in a steady state and the turbulent dynamo balances the resistive diffusion term in the outer part of the domain, whereas the pinch velocity term is more important in the inner part. At the end of the transient PPCD phase, when the fluctuations are highly depressed, the increase of the toroidal flux in the core is related to a negative poloidal electric field and to a large pinch velocity term. This picture differs from the original one of a resistive diffusion of the current from the plasma edge during PPCD.

The analysis of the modification of the mode spectrum induced by PPCD at different radial positions shows that, while at the edge all the $m = 1$ modes decrease, near the axis some of the amplitudes increase or only slightly decrease (figure 11). This could explain the experimental observation that in several discharges a thermal structure is observed in the plasma core, but a corresponding dominant mode is not detected by the external magnetic measurements [10]. To some extent this radial behaviour characterizes also the relative variation of more global quantities when comparing edge and internal values (edge variations are in general more sensitive to the external action). For example, in correspondence with the case shown in figure 11, the total rms value of the toroidal field at the edge and the volume integral of the magnetic perturbation energy vary during PPCD as $\delta Bz_{\mathrm{beforePPCD}}/\delta Bz_{\mathrm{afterPPCD}} = 2.6$ and $\delta E^{\mathrm{M}}_{\mathrm{beforePPCD}}/\delta E^{\mathrm{M}}_{\mathrm{afterPPCD}} = 4.1$. This reduction of the magnetic perturbation is quantitatively consistent with the experimental one and with the reduction of the stochastic diffusion as estimated in the next paragraph.

Finally, it can be observed that PPCD acts so as to increase the pinch parameter (RFX Θ: $1.4 \rightarrow 1.7$, F: $-0.1 \rightarrow -0.5$; SpeCyl PPCD Θ: $1.6 \rightarrow 2.1$, F: $-0.1 \rightarrow -0.6$) so that the system in its evolution tries to reach conditions characteristic of high Θ stationary regimes. In this respect we could also interpret the behaviour of the mode energy itself: numerical simulations [17] and experimental results [18] have previously indicated a decrease of the $m = 1$ mode energy content in high Θ conditions. At the same time the significant increase of the $m = 0$ component observed at high Θ occurs only on a longer timescale in the simulations of PPCD. This may be explained by the fact that their amplitude is a balance between the nonlinear drive by $m = 1$ modes and linear destabilization effects: further investigations will address this feature.

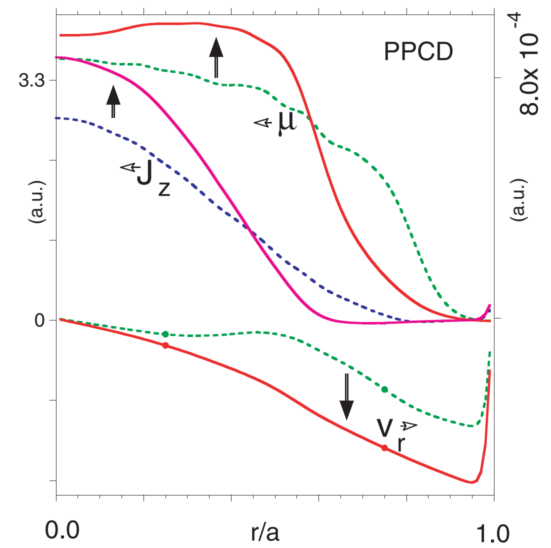

Figure 9. Comparison of the profiles of the toroidal current density, of $\mu = J \cdot B/B^2$, and of the radial velocity obtained from the three-dimensional simulation before and at the end of PPCD.

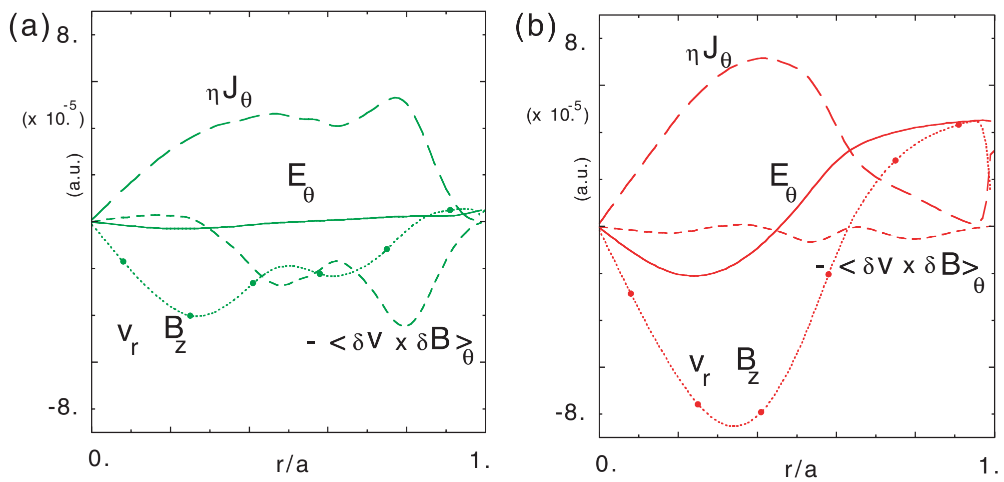

Figure 10. Profile of E_Θ and of its three components before (*a*) and at the end (*b*) of PPCD.

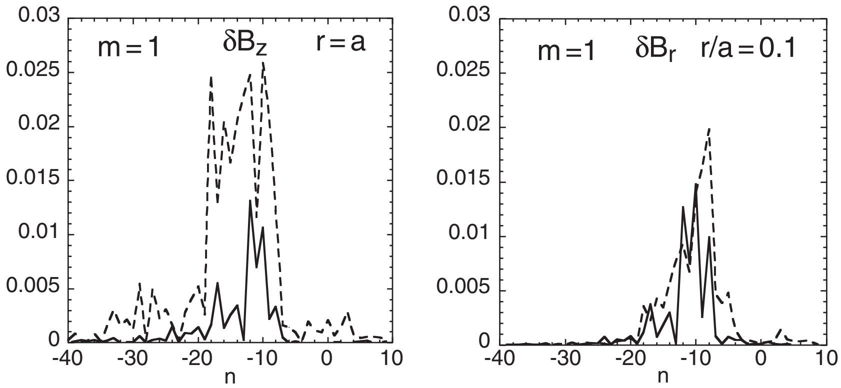

Figure 11. $m = 1$ mode spectrum before (- - - -) and during (——) PPCD at $r = a$ (left) and at $r/a = 0.1$ (right).

4. Transport simulations

Analysing the time behaviour of the F–Θ parameters in RFX, it was noted [19] that during PPCD except for a short initial interval of 1 ms or less, the magnetic profiles evolve as if there were an anomalous vacuum-like diffusion of the external B_ϕ perturbation in the plasma. This was explained assuming a prompt reduction of the dynamo action that compensates the increase of toroidal flux induced by the additional poloidal current applied at the edge region. This observation finds good correspondence with the decrease in dynamo activity and the increase in pinch convection described in the previous section. Taking into account these results, to look in a more quantitative way at the transport problem, a one-dimensional time-dependent transport code (RFXPORT, [20]) has been applied that solves the equations for the evolution of the magnetic profiles together with the temperature profile. In the model the parallel component of the dynamo electric field is included as an 'ad hoc' term, $\boldsymbol{E}_\mathrm{d}(r) = \alpha(r)\boldsymbol{B}(r)$. In particular, $\alpha(r)$ is determined by requiring stationarity of the magnetic profiles before application of PPCD, and its profile is assumed unchanged during the PPCD phase. At present, a perpendicular component of the dynamo field is not included in the code, while it is present in the three-dimensional numerical simulations. This term could in principle affect the radial velocity profile.

A simulation of PPCD has been done by applying the consistent boundary conditions and by reducing the α function by 50% all along the minor radius. A peaking of the current profile is found as in the three-dimensional simulation, though transport is not present in the three-dimensional code.

The transport code also reproduces the experimental variation of temperature with a thermal diffusivity, χ, decreasing during PPCD from $\sim$500 to $\sim$100 $\mathrm{m^2\,s^{-1}}$ in the plasma core (figures 12 and 13). This decrease is consistent with a stochastic diffusion dependence as $\chi \sim (\delta B/B)^2$ [2, 21] and with the fluctuation reduction observed experimentally and in three-dimensional MHD simulations. If a milder reduction of the dynamo field is used in the one-dimensional model, the F parameter deviates more from the experimental one. In figure 14 the evolutions of F and Θ obtained by reducing E_d by 50% and 30% are compared with the experimental curves. Indeed the value of Θ remains somewhat higher than the experimental in both cases, but when E_d is reduced only by 30% the F parameter reaches too large negative values.

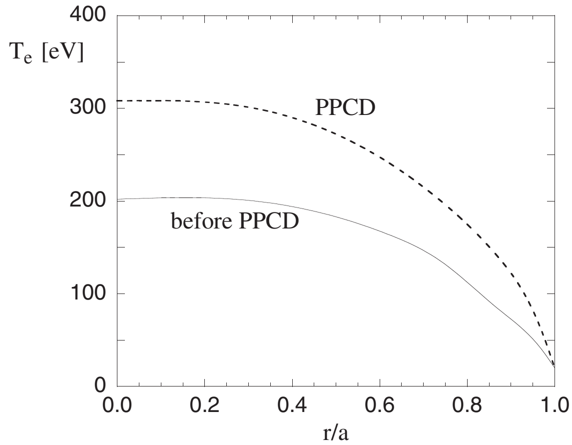

Figure 12. Electron temperature profiles as obtained by the one-dimensional transport model RFXPORT before and during PPCD.

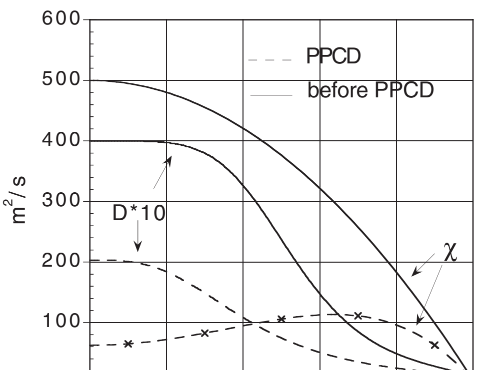

Figure 13. Thermal diffusivity and particle diffusion coefficient used to simulate, respectively, the temperature (RFXPORT) and density (particle diffusion model) behaviour in stationary conditions and during PPCD.

The apparent lack of significant effects of PPCD on the density profiles of RFX could appear to be in contrast with a regime of reduced transport. Indeed, in the MST experiment, significant increase in density and large improvements of particle confinement have been reported during PPCD [22, 23].

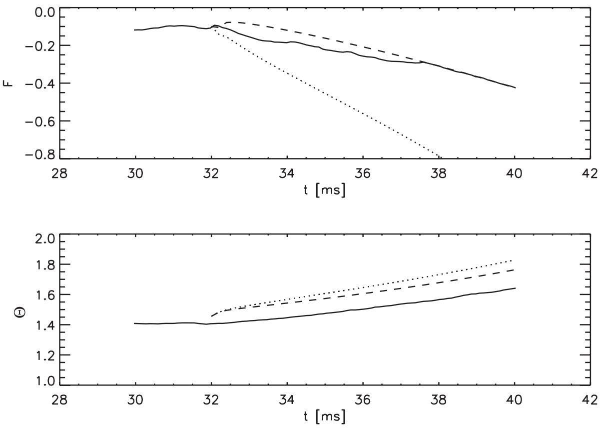

Figure 14. Time behaviour of the $F = B_\Phi(a)/\langle B_\Phi\rangle$ and $\Theta = B_\Theta(a)/\langle B_\Phi\rangle$ parameters as obtained from the experiment and from the one-dimensional code RFXPORT. (——): experimental; (- - - -): E_d reduced by 50%; (· · · · · ·): E_d reduced by 30%.

On the other hand, some important differences between the RFX and the MST experiments have to be considered. First, the reduction by means of the PPCD of the macroscopic magnetic perturbation due to the locked dynamo modes and the associated reduction of the influxes from the wall are effects much less important in MST than in RFX. This is mainly because the former has a close fitting aluminium shell coinciding with the first wall that greatly reduces the radial field at the wall and does not trap large amounts of hydrogen. Moreover, due also to the highly recycling graphite first wall, RFX typically operates at higher densities compared with MST, which entails a much shallower penetration of the neutrals, i.e. the source profile in RFX is much more edge peaked than for MST. Therefore, a reduction of the transport coefficient in the core region, where the source term is negligible, has little effect on the density profile in RFX. At the same time, the large reduction of the influx during PPCD results in a transient decrease of density.

These qualitative arguments have been quantitatively studied using a one-dimensional cylindrically symmetric transport code in a predictive scheme [16]. The particle flux is expressed as

$$\Gamma = \Gamma_{an} + \Gamma_0 = -(D_{an} + D_{el})\nabla n + v_{an}\cdot n + v_{E\times B}\cdot n,$$

where D_{el} is a term added to the diffusion coefficient to account for the electrostatic transport at the edge. D_{an} and v_{an} are related by $v_{an} = -D_{an}\nabla T_e/2T_e$ according to the stochastic ambipolar diffusion model [24]. We have used the same method as in [16]: free parameters D_{an} and D_{el} are adjusted with the criterion that the simulations are not considered acceptable if their χ^2 relative to the line integral measurements does not lie within the confidence region determined by the inversion procedure. The quality of the agreement between the simulations and the experimental data is highlighted in figure 15.

As with what was found in the past [16], the stationary pre-PPCD density profile can be reproduced with a diffusion coefficient of the order of $40\,m^2\,s^{-1}$ in the centre decreasing to $1\,m^2\,s^{-1}$ at the edge (figure 13). Impurities could contribute as an electron source [25]. However, their effect has been neglected, as discussed in [16], due to the low-charge ions

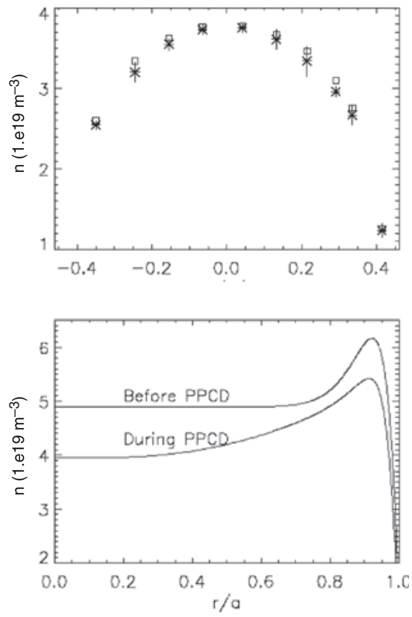

Figure 15. Top: experimental line average electron densities measured during PPCD along 10 chords (∗) compared with the simulation by the one-dimensional particle diffusion code (□). Bottom: simulation of the electron density profiles obtained by the particle diffusion code before and during PPCD.

present in RFX (carbon and oxygen), resulting in a low effective charge, which does not increase during PPCD. Consistent with the experimental decrease of total hydrogen influx, during PPCD the source term in the particle continuity equation, i.e. the neutral density, has been decreased by a factor of 2. Then a good simulation of the density profile (see figure 15) can be obtained assuming a decrease of D_{an} by a factor $\leqslant 2$ during PPCD (figure 13). A lower diffusion coefficient would imply a more peaked density profile both directly by the term $D_{an}\nabla n$ and through the dependence of the outward velocity. These effects are substantially compensated by the higher temperature gradient (resulting in a net increase of the anomalous outward velocity) and by the reduced source. In this way a hollow density profile with decreasing total number of particles is maintained. Therefore, the very different behaviours of the n_e and T_e profiles in RFX are both consistent with a reduced diffusion regime. It can be observed that, both before and during PPCD, the χ/D ratio is ∼5–10, while the value expected from the collisionless Rechester and Rosenbluth model would be $\chi/D = (m_e/m_i)^{1/2} \approx 40$. On the other hand, due to the uncertainty in the estimates of the source term and the local T_e gradient and to the relatively small gradients that characterize the core density profiles in RFX, it is presently rather difficult to draw a definite conclusion on behaviour of particle diffusivity during PPCD. Actually, the particle transport mechanisms in RFX are still a matter of debate. For example, considering collisional effects, which can play a role especially at the plasma edge, would imply a lower value for χ/D [21].

5. Combined pellet–PPCD experiments

A perturbed transport study [26] has been performed launching hydrogen pellets in combination with PPCD. The pellets had

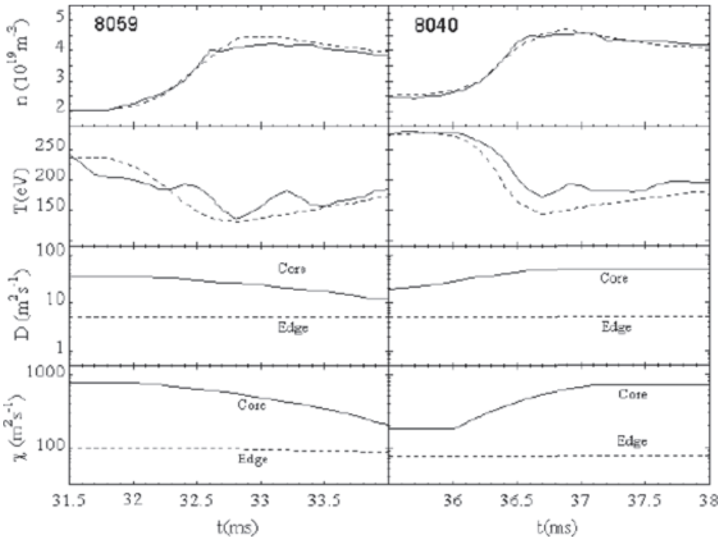

Figure 16. Experimental (——) and simulated (- - - -) central density and temperature, simulated central and edge D, and χ for shots 8059 and 8040.

a velocity $v_p = 400$–$500\,\mathrm{m\,s^{-1}}$ and ablated completely in the plasma: they reached the centre and produced a transient peaking of the density profile. The volume average density was roughly doubled, whereas the central temperature was reduced by 30–40%. In standard discharges pellets reaching the plasma centre trigger a dynamo relaxation event that enhances the global transport and prevents temperature recovery after injection [27]. This is thought to be induced by the strong core cooling with the associated growth of centrally resonating MHD modes. Conversely, injecting a pellet during PPCD, we find that two cases are possible, depending on the relative timing between pellet and PPCD. If the pellet is injected in the early phase of the PPCD when its mode stabilizing effect is strong enough, a synergy between pellet injection and PPCD is seen: the plasma-enhanced confinement is maintained, leading to an increase of the global β. This is shown in figure 16 (pulse 8059). In this case PPCD starts at 32 ms, at the same time that the pellet enters the plasma. Both D and χ decrease, as in successful PPCD experiments unperturbed by pellets. On the other hand, for pellet injected at later times, the PPCD is less effective and the transport reduction is lost (figure 16 pulse 8040, PPCD starts at 32 ms, pellet enters the plasma at 36 ms). These results confirm the robustness of the improved confinement regime, which is resilient to large density and temperature perturbations in the plasma core.

6. Summary and conclusions

The simulation with a nonlinear three-dimensional MHD code confirms the concentration and peaking of the magnetic and current density profiles obtained by simple equilibrium reconstruction models applied to RFX data and also experimentally found in MST by direct FIR measurements of the toroidal component of the current density [28]. In our analysis this effect is essentially due to the decrease of the turbulent dynamo term and to the increase of the pinch velocity associated with the toroidal flux modifications. At variance with what was originally proposed as an explanation for the perturbation reduction during PPCD [1, 7], these results indicate that the PPCD action does not produce a net current drive in the edge plasma region. In particular, an improvement in terms of linear stability is not found—which would require a flattening of the parallel current density profile [29]. This may not be a surprise, since in highly nonlinear systems, like the RFP, the saturation amplitude of the perturbations is not expected to be primarily determined by the linear stability. Further analysis will address this issue.

One-dimensional time-dependent transport codes show that a thermal diffusivity decreasing during PPCD proportionally to $(\delta B/B)^2$ explains the experimentally observed temperature increase and peaking. A decrease of the particle diffusion is also consistent with the experimental density profiles, although not completely consistent with the stochastic model.

The general picture of a PPCD experiment in RFX emerging from our analysis is the following. The externally driven increase of the toroidal field reversal produces a drop in the magnetic fluctuations and a concentration of the toroidal flux in the core. In this condition the non-stationarity of the system makes unnecessary the symmetry breaking of a stationary Ohmic device (Cowling theorem, [30]). Consequently transport is reduced, T_e increases, and the magnetic and temperature profiles peak.

The combined pellet–PPCD experiments have further confirmed this picture, showing that a robust improved confinement is present only during the early phase of PPCD, when the amplitude of the MHD modes is quenched.

Although several issues remain open and a more quantitative assessment of the process would require a better knowledge of the experimental magnetic and plasma profiles, the link between transport and magnetic turbulence is confirmed by our analysis. We also remark that in different machines different configurations and operational regimes may correspond to different physical processes. In any case, when estimating global confinement times the caveat regarding the highly transient conditions should be considered [1, 23, 31, 32].

A possible technique to extend the reduced dynamo phase is the application of an oscillating poloidal electric field at the plasma edge. Experiments performed in RFX demonstrated that, despite being intrinsically transient, the inductive current drive leads to an improved regime if applied in a repetitive scheme [14]. Another possibility of obtaining a steady state without magnetic turbulence is that of an Ohmic single helicity state [33], though yet to be experimentally achieved. Alternatively, non-magnetic techniques such as the RF current drive [31] could be experimented in RFPs to demonstrate the attainability of a stationary low turbulence regime.

References

[1] Bartiromo R. *et al* 1999 *Phys. Rev. Lett.* **82** 1462
[2] Rechester A.B. and Rosenbluth M.N. 1978 *Phys. Rev. Lett.* **40** 38
[3] Escande D.F. *et al* 2000 *Phys. Rev. Lett.* **85** 1662
[4] Antoni V. 1997 *Plasma Phys. Control. Fusion* **39** B223
[5] Zanca P., Bettella D., Martini S. and Valisa M. 2001 *J. Nucl. Mater.* **290–293** 990
[6] Valisa M. *et al* 1997 *J. Nucl. Mater.* **241–243** 988
[7] Sarff J.S. *et al* 1994 *Phys. Rev. Lett.* **72** 3670
[8] Chapman B.E. *et al* 2000 *Phys. Plasmas* **7** 3491
[9] Yagi Y. *et al* 2002 *Plasma Phys. Control. Fusion* **44** 335
[10] Cravotta A. *et al* 2003 *Phys. Plasmas* **10** 705
[11] Antoni V. *et al* 2000 *Plasma Phys. Control. Fusion* **42** 893
[12] Carraro L. *et al* 2002 *Plasma Phys. Control. Fusion* **44** 2135
[13] Bolzonella T. *et al* 1997 *24th EPS Conf. on Control. Fusion and Plasma Physics (Berchtesgaden, 1997)* vol 1 (EPS) p 321
[14] Bolzonella T. *et al* 2001 *Phys. Rev. Lett.* **87** 195001
[15] Martin P. *et al* 2000 *Phys. Plasmas* **7** 1984
[16] Gregoratto D. *et al* 1998 *Nucl. Fusion* **38** 1199
[17] Cappello S. and Biskamp D. 1996 *Nucl. Fusion* **36** 571
[18] Hirano Y., Maejima Y., Shimada T., Hirota I. and Yagi Y. 1996 *Nucl. Fusion* **36** 721
[19] Martini S., Terranova D., Innocente P. and Bolzonella T. 1999 *Plasma Phys. Control. Fusion* **41** A315
[20] Cappello S. *et al* 1989 *Int. Conf. on Plasma Phys. (New Delhi, 1989)* vol III, p 881
[21] D'Angelo F. and Paccagnella R. 1999 *Plasma Phys. Control. Fusion* **41** 941
[22] Sarff J.S., Lanier N.E., Prager S.C. and Stoneking M.R. 1997 *Phys. Rev. Lett.* **78** 62
[23] Chapman B.E. *et al* 2002 *Phys. Plasmas* **9** 2061
[24] Harvey R.W. *et al* 1981 *Phys. Rev. Lett.* **47** 102
[25] Lanier N.E. *et al* 2000 *Phys. Rev. Lett.* **85** 2120
[26] Lorenzini R. *et al* 2002 *Plasma Phys. Control. Fusion* **44** 233
[27] Garzotti L. *et al* 1997 *24th EPS Conf. on Control. Fusion and Plasma Physics (Berchtesgaden, 1997)* vol 1 (EPS) p 313
[28] Brower D.L. *et al* 2002 *Phys. Rev. Lett.* **88** 185005
[29] Cappello S., Paccagnella R. and Ortolani S. *30th EPS Conf. on Control. Fusion and Plasma Physics (St Petrsburg, 7–11 July 2003)* vol 27A (ECA) P-1.201
[30] Cowling T.G. 1934 The magnetic field of sunspots *Mon. Not. R. Astron. Soc.* **94** 39–48
[31] Sarff J.S. *et al* 2002 Overview of improved confinement and plasma control in the MST reversed field pinch *Proc. 19th Int. Conf. on Fusion Energy 2002 (Lyon, 2002)* (Vienna: IAEA) CD-ROM file OV/4-3 and http://www.iaea.org/programmes/ripc/physics/fec2002/html/fec2002.htm
[32] Sakakita H. *et al* 2002 Active MHD instability control and confinement in the TPE-RX RFP *Proc. 19th Int. Conf. on Fusion Energy 2002 (Lyon, 2002)* (Vienna: IAEA) CD-ROM file EX/P2-07 and http://www.iaea.org/programmes/ripc/physics/fec2002/html/fec2002.htm
[33] Escande D.F. *et al* 2000 *Plasma Phys. Control. Fusion* **42** B-243